Translational Oncology
www.transonc.com

Volume 12 Number 3 March 2019 pp. 432–440 432

# Up-Regulated FGFR1 Expression as a Mediator of Intrinsic TKI Resistance in EGFR-Mutated NSCLC

**Kristine Raaby Gammelgaard[*,†], Johan Vad-Nielsen[*], Michelle Simone Clement[†], Simone Weiss[*], Tina Fuglsang Daugaard[*], Frederik Dagnæs-Hansen[*], Peter Meldgaard[‡], Boe Sandahl Sorensen[†] and Anders Lade Nielsen[*]**

[*]Department of Biomedicine, Aarhus University, Aarhus, Denmark; [†]Department of Clinical Biochemistry, Aarhus University Hospital, Aarhus, Denmark; [‡]Department of Oncology, Aarhus University Hospital, Aarhus, Denmark

## Abstract

Non-small cell lung carcinoma patients with epidermal growth factor receptor (EGFR) mutations are offered EGFR tyrosine kinase inhibitors (TKI) as first line treatment, but 20–40% of these patients do not respond. High expression of alternative receptor tyrosine kinases, such as Fibroblast growth factor receptor 1 (FGFR1), potentially mediates intrinsic EGFR TKI resistance. To study this in molecular detail, we used CRISPR-dCas9 Synergistic Activation Mediator (SAM) for up-regulation of *FGFR1* in physiological relevant levels in the EGFR mutated NSCLC cell lines HCC827 and PC9 thereby generating HCC827$^{gFGFR1}$ and PC9$^{gFGFR1}$. The sensitivity to the TKI erlotinib was investigated *in vitro* and in a BALBc nu/nu mouse xenograft model. FGFR1 up-regulation decreased TKI-sensitivity in both NSCLC cell lines in the presence of the ligand fibroblast growth factor 2 (FGF2). Xenografts were established with PC9$^{gFGFR1}$ cells and it was demonstrated that there was no significant difference in tumor size between TKI- and vehicle-treated PC9$^{gFGFR1}$ tumors. This supports decreased TKI-sensitivity in NSCLC cells with FGFR1 up-regulation. Our study points to FGFR1 signaling being an intrinsic resistance mechanism abolishing TKI response in EGFR mutated NSCLC.

*Translational Oncology (2019) 12, 432–440*

## Introduction

Non-small cell lung cancer (NSCLC) is the leading cause of cancer-related mortality worldwide [1]. NSCLC is often diagnosed in the metastatic or unresectable setting, while patients undergoing potentially curative surgery frequently relapse [2]. The introduction of molecularly targeted agents in NSCLC therapy was a major breakthrough in treatment of patients harboring activating genetic alterations including EGFR, anaplastic lymphoma kinase (ALK), and proto-oncogene tyrosine-protein kinase ROS (ROS1) [3–5]. Patients with *EGFR* mutations are now offered EGFR TKIs as first line treatment [6–9], but in 20–40% of the patients, a treatment response is absent [10]. In patients exhibiting this intrinsic resistance short term stable disease is the most favorable outcome [11].

Decreased Bcl-2-like protein 11 *(BIM)* mRNA expression, *EGFR*-polymorphisms, and resistance mutations in *EGFR* [10,12,13] are associated with intrinsic resistance to EGFR TKI in EGFR mutated patients, but so far the impact of alternative activated receptor tyrosine kinases (RTK) remains unsettled. *FGFR1* gene-amplification was associated with intrinsic resistance to gefitinib [14] but this was in an EGFR WT xenograft model. Lenti-viral induced overexpression of FGFR1 in PC9 NSCLC cells resulted in insensitivity to the EGFR TKI gefitinib *in vitro* [15]. Furthermore, others and we have described FGFR1 up-regulation as an acquired resistance mechanism to EGFR TKI treatment [16–19]. Acquired resistance occurs under therapeutic selective pressure and may result in multiple simultaneous and interacting resistance mechanisms as previously reported [19].

Address all correspondence to: Professor MSO Anders Lade Nielsen, MSc, PhD, Department of Biomedicine, Bartholins allé 6, Bartholin bld. 1242, DK-8000 Aarhus C, Denmark.
E-mail: aln@biomed.au.dk
Received 5 October 2018; Revised 27 November 2018; Accepted 27 November 2018


1936-5233/19
https://doi.org/10.1016/j.tranon.2018.11.017

Further studies focusing on the erlotinib-naïve situation is hence needed to elucidate the role of FGFR1 mediated resistance as a player in intrinsic resistance.

FGFR1 is activated through binding of FGF ligand. A total of 18 different FGF ligands exist [20,21], and FGF2 has been described as a potent inducer of FGFR1-mediated acquired EGFR TKI resistance in several studies [16–18]. A recent report suggested that in FGF2 activated FGFR1-amplified NSCLC cell lines, FGFR1 drives proliferation through the extracellular-signal-regulated kinase (ERK) pathway [22]. This has, however, not been investigated in relation to FGFR1 up-regulation and intrinsic EGFR TKI sensitivity.

In this study, we have investigated the impact of up-regulation of *FGFR1* gene expression alone or in combination with FGF2 in accordance to intrinsic EGFR TKI resistance mechanism in EGFR mutated NSCLC *in vitro* and in a xenograft mouse model.

## Materials and Methods

### *Compliance with Ethical Standards*

All experiments were conducted under the required approvals from the Danish Ethical Research Committees (Project 1–10–72-215-17).

### *Cell Culture*

HCC827 (ATCC/LCG, Wesel, Germany) and PC9 (PHE culture collection, Salisbury, UK) cells were grown in RPMI supplemented with 10% fetal calf serum and 1% Penicillin–streptomycin (Gibco, Thermo Fischer Scientific, Waltham, MA, USA). The cells were grown at 37 °C and 5% $CO_2$.

### *Generation of Stable Cell Lines*

*FGFR1* gene expression was genetically up-regulated using a CRISPR-dCas9 SAM (Supplemental Figure S1) [23]. CRISPR-dCas9 transduction: Lenti-viral constructs containing dCas9-vp64 (lenti dCAS-VP64_Blast, addgene) and MS2-P65-HSF1 (lenti MS2-P65-HSF1_Hygro, addgene) were prepared using HEK293T cells and frozen until further use. A total of 300,000 HCC827 or PC9 cells were seeded in each well in a 6-well tray the day before transduction. On the day of transduction 0.75 mL dCas9-vp64 crude virus and 0.75 mL MS2-P65-HSF1 crude virus was added with 1.5 mL of media with a final polybrene concentration of 8 μg/mL. Selection was performed using blasticidin (0.5 μg/mL, Gibco) and hygromycin (200 μg /mL, Life Technologies). For stable transfection with multiplexed gRNA PiggyBag Transposon vectors three unique SAM compatible gRNAs spanning the promoter region of *FGFR1* (T1–3) were assembled into a single vector as described previously [24,25]. This generated the expression vector gFGFR1. Briefly, the three gRNAs were assembled into separate expression vectors (pMA-T1 SAM, pMA-T2 SAM and pMA-T3 SAM). gRNA sequences are presented in Supplemental Table 1. The gRNA vectors were ligated into a pFUS-B3 vector and further assembled with a pFUS-A vector into a PiggyBag transposon vector containing the BsmBI sites of the MsgRNA vector, denoted pPBT/CAIP-MsgRNA. The transposon cassette also contained sequences encoding AsRed and puromycin resistance gene. A *mCherry* gRNA was used in all three positions to generate the gRNA expression vector gCTR. Vector maps are presented in Supplemental Figure S2.

For stable transfection, 900 ng of pPBT/CAIB-MsgRNA (gFGFR1 or gCTR) was mixed with 100 ng of HypBase vector and 3 μL of X-treme gene 9-transfection agent (Sigma Aldrich, St. Louis, MO, USA). After 30 min of incubation the transfection mix was added to recipient cells and left to incubate for 24 h. Selection was started after 2 days using puromycin (1 μg/mL for PC9 and 0.5 μg/mL for HCC827). Transfection with gFGFR1 and gCTR was performed simultaneously to generate HCC827$^{gFGFR1}$, HCC827$^{gCTR}$, PC9$^{gFGFR1}$, and PC9$^{gCTR}$. The cells were grown without selection during protein harvesting and MTS assays, but kept under selecting conditions otherwise.

### *Western Blotting*

Protein concentration was determined using the BCA quantitation assay (Thermo Fisher Scientific, Waltham, MA, USA) and loaded on a NuPage 4–12% Bis-Tris gel (Thermo Fisher Scientific, Waltham, MA, USA). The gel was blotted onto a PVDF membrane and the membrane was concurrently blocked with 5% skimmed milk. The membrane incubated with primary antibody with rotation ON at 4 °C, and hereafter incubated with secondary antibody for 1 h before development with ECL, SuperSignal West Dura Extended Duration Substrate (Thermo Fisher Scientific, Waltham, MA, USA) using the ImageQuant LAS 4000 system (GE Healthcare Life Sciences, Little Chalfont, UK). Antibody information is available in Supplemental Table 2.

### *qPCR*

RNA extraction was performed using TRI Reagent according to manufacturer's instructions (Sigma-Aldrich, St. Louis, MO, USA). cDNA was prepared with iScriptTM cDNA Synthesis Kit according to manufacturer's instructions (Bio-Rad, Hercules, CA, USA). qPCR experiments were run in triplicates of 10 μL consisting of 0.125 μL forward primer (10 pmol/μL), 0.125 μL reverse primer (10 pmol/μL), 3.750 μL RNase-free water, 5 μL SYBR green (Roche, Bassel, Switzerland) and 1 μL cDNA. qPCR was performed on a Roche Lightcycler 480 with the following settings: heating at 95 °C for 15 min, 45 cycles of PCR (95 °C 10 sec, 58 °C 20 sec, 72 °C 15 sec) and final elongation at 72 °C for 1 min. Normalization to *Beta-actin* was performed using the X0 method [26]. Primer sequences are available in Supplemental Table 3.

### *Inhibitor Assays*

For MTS analysis of drug sensitivity, 1000–5000 cells were plated in each well in a 96-well plate with 100 μL media. Each sample was measured in a minimum of 4 replicates including a media control sample. 20 ng/mL FGF2 (cat. no. 130–093-837, Miltenyi, Bergisch Gladbach, Germany) was added on day 1 and again together with the inhibitor on day 2. The cells were treated with the indicated inhibitor for 72 h before MTS mixture was added according to the manufacturer's instructions (CellTiter 96 AQueous Non-Radioactive Cell Proliferation Assay, Promega, Madison, WI, USA).

Erlotinib and AZD4547 were obtained through Selleckchem (Houston, TX, USA). A broad range of concentrations were tested before a range was selected for testing on all cell lines.

### *Xenograft Experiments*

Animal experiments were conducted in accordance with a permit from the National Authority on Animal experiments (2017-15-0201-01170). Thirty female 6–8 week old BALBc nu/nu mice (BALB/cAnNRj-*Foxn1*$^{nu/nu}$) were purchased (Janvier-Labs, Le Genest-Saint-Isle, France.

France) and allowed to acclimatize for 1 week. The mice were kept under SPF conditions in filtertop cages with continuous access to

food and water. The tumor size and weight of the mice were determined every 2–3 days with caliper and the mice were sacrificed at a weight-loss >20% or tumor size beyond 1000 $mm^3$.

A total of 5*10^6 PC9 cells were inoculated into the flank of each mouse. The cells were solubilized in 100 µL PBS containing 50% matrigel (Corning, Thermo Scientific, Waltham, MA, USA). The tumor growth was monitored every 2–3 days, and when the tumor reached 100–200 $mm^3$, the mouse was randomized to either erlotinib (n = 8) or captisol (vehicle) (n = 7). All groups (n = 4) had comparable mean tumor size. The mice were treated with 50 mg/kg erlotinib or 100 µL vehicle every day (except weekends) for 3 weeks.

The tumors were measured with caliper every 2–3 days throughout the experiment. Tumor volume was calculated based on the formula: width^$^2$ × length × 0.5. To adjust for the contribution of skin 0.5 mm was subtracted from width and length measurements. For *in vivo* imaging, mice were anesthetized with inhaled isoflurane and were maintained with 2–3% isoflurane during imaging procedures. AsRed fluorescent imaging was performed with an IVIS200 imaging system equipped with a camera box and warming stage. Images were captured and tissue autofluorescence subtracted by spectral unmixing. Pictures were generated using Living Image 3.2 acquisition and analysis software (Caliper Life Sciences, Hopkinton, MA).

For preparation of Erlotinib for oral gavage 100 mg Erlotinib (cat no. S1023, Selleckchem, Houston, TX, USA) was solubilized in 15% Captisol (Captisol, San Diego, CA, USA) with sonication and heating at 50 °C for 10 min for a final concentration of 10 mg/mL. Captisol 15% was used for vehicle treatment; 100 µL per mouse was used for oral gavage.

### *FGF2 ELISA*

For FGF2 ELISA for EGFR mutated patients serum was collected from patients with advanced NSCLC, harboring an EGFR mutation, and treated with erlotinib at the Department of Oncology, Aarhus University Hospital (from a previously described study of patients [7], and approved by the national health research committee, 1–10–72-215-17). ELISA was performed on 36 serum samples. FGF2 was quantified in duplicates of 100 µL serum with Quantikine HS ELISA kit for Human FGF basic Immunoassay (cat nr. HSFB00D, R&D, Minneapolis, MN, USA). The samples were diluted 1:2 in assay dilution buffer. The background cut-off was defined as the optical density of the blanks +3 × SD. None of the patient samples were below the cut-off.

For FGF2 ELISA for Xenograft tumor samples resected tumor tissue from the xenograft experiments was homogenized in 300–500 µL of PBS with protease inhibitors (cOmplete mini, Roche Bassel, Switzerland) and resolved in equal amounts of Cell Lysis buffer 2 (R&D, Minneapolis, MN, USA). Tissue lysates were diluted 1:20 in calibrator dilution buffer (MFB00, R&D, Minneapolis, MN, USA) prior to performing the ELISA. FGF2 was quantified in duplicates of 50 µL diluted tissue lysate with Mouse/Rat FGF basic Quantikine ELISA kit (MFB00, R&D, Minneapolis, MN, USA). The background cut-off was defined as the optical density of the blanks +3 × SD. No samples were below the cut-off.

### *Statistics*

Inhibitor assays measured with MTS was compared using multiple *t*-tests with Holm-Sidak correction for multiple comparisons. To compare tumor volumes measured during vehicle or erlotinib treatment of $PC9^{gFGFR1}$ and $PC9^{gCTR}$, we performed a repeated measurement ANOVA using Sidak's multiple comparisons test. Final tumor weight and volume within the groups were compared using an unpaired *t*-test. For mice undergoing at least 2 weeks of erlotinib-treatment, which were withdrawn before the end of the experiment due to wounds (n = 2), linear regression was performed and a final tumor volume was extrapolated. Correlation between final tumor volume and FGF2 levels were performed using Pearson's correlation coefficient test. Comparison of PFS and OS based on median FGF2 levels in patients were performed using a paired *t*-test. Analyses were

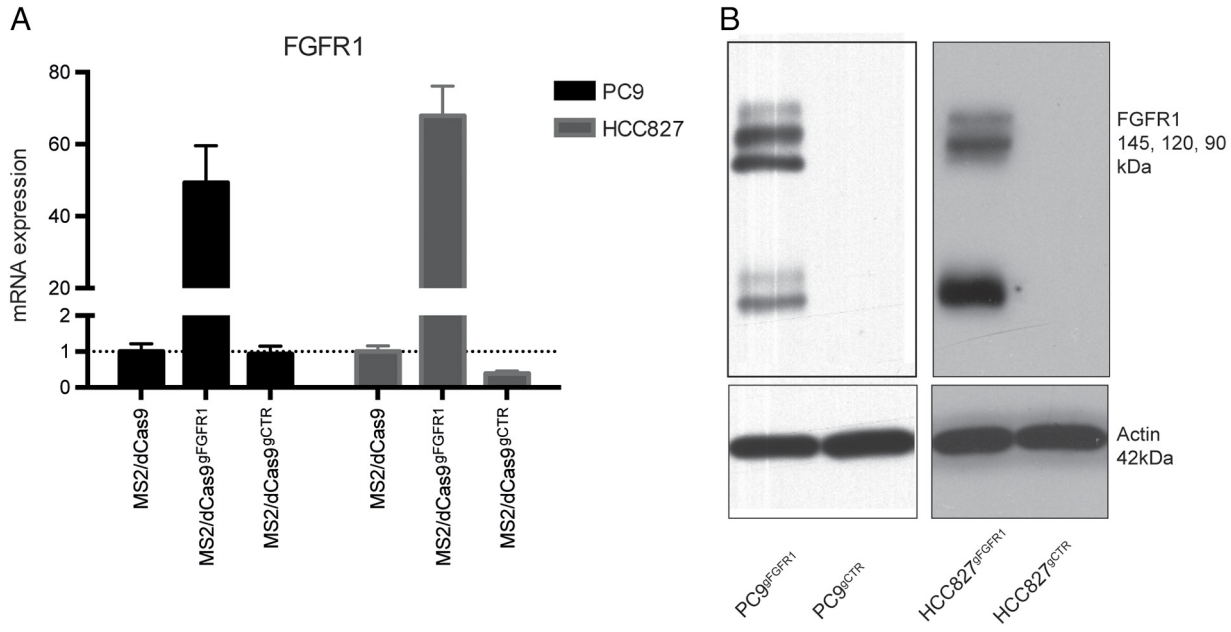


**Figure 1.** FGFR1 expression in cells with dCAS9-vp64 and MS2-p65-HSF-1 background alone or with stable transfection of gFGFR1 or gCTR. A. *FGFR1* mRNA expression normalized to *beta-actin*. B. Western blotting of FGFR1 in PC9 and HCC827 gFGFR1 and gCTR cells (N = 2).

performed using Graphpad Prism 6 and Excel 2011. *P* values <.05 were considered significant.

## Results

### *Generation of NSCLC Cell Lines with FGFR1 Up-Regulation Using CRISPR-dCas9 SAM*

We utilized the CRISPR-dCas9 SAM approach (Supplemental Figure S1) [23] in order to investigate the effect of up-regulated *FGFR1* gene expression in EGFR mutated NSCLC cell lines. PC9 and HCC827 cells with stable expression of dCas9-vp64 and MS2-p65-HIF-1 were established using lenti-viral vectors. For *FGFR1* up-regulation, three different gRNAs complementary to the *FGFR1*-promoter were designed (Supplemental Table 1) and assembled into a single vector [25]. PC9 and HCC827 with dCas9-vp64 and MS2-p65-HIF-1 were subsequently transfected with *FGFR1*-specific gRNAs or control (CTR) gRNAs targeting mCherry. $PC9^{gFGFR1}$, $HCC827^{gFGFR1}$, $PC9^{gCTR}$, and $HCC827^{gCTR}$ cell lines were established with stable expression of gRNAs.

qPCR analysis revealed a 50-fold up-regulation of *FGFR1* mRNA in both $PC9^{gFGFR1}$ and $HCC827^{gFGFR1}$ compared to $PC9^{gCTR}$ and $HCC827^{gCTR}$ (Figure 1*A*). FGFR1 protein levels were also up-regulated in $PC9^{gFGFR1}$ and $HCC827^{gFGFR1}$ compared to $PC9^{gCTR}$ and $HCC827^{gCTR}$ (Figure 1*B*). To check for gRNA specificity, we performed qPCR to analyze mRNA expression for *FGFR2* and *FGFR3*. There were undetectable levels of *FGFR2* and *FGFR3* mRNA both before and after introduction of *FGFR1* gRNAs in qPCR experiments (data not shown).

### *FGFR1 Up-Regulation and TKI-Sensitivity*

We then investigated the impact of FGFR1 up-regulation on EGFR TKI-sensitivity using an MTS-based proliferation assay. Under standard cell growth conditions, there was no difference in sensitivity to erlotinib in $PC9^{gFGFR1}$ and $HCC827^{gFGFR1}$ compared to $PC9^{gCTR}$ and $HCC827^{gCTR}$, respectively (Figure 2*A*). Since FGFR1 signaling is activated upon ligand binding, FGFR1 may be highly expressed but not activated. Hence, we stimulated the cells with 20 ng/mL FGF2 24 h before and during erlotinib treatment. The addition of FGF2 significantly decreased the erlotinib-sensitivity of $PC9^{gFGFR1}$ and $HCC827^{gFGFR1}$ compared to $PC9^{gCTR}$ and $HCC827^{gCTR}$, respectively (Figure 2*B*). To decrease the influence of growth factors present in serum, we performed the assay under conditions of serum starvation (0.5% FCS). Under these conditions the effect of FGF2 was pronounced for $PC9^{gFGFR1}$ and $HCC827^{gFGFR1}$ compared to $PC9^{gCTR}$ and $HCC827^{gCTR}$, respectively (Figure 2, *C* and *D*). We evaluated if the change in erlotinib-sensitivity was specific to FGF2 by performing erlotinib treatment with the presence of FGF1. This revealed a decrease in erlotinib-sensitivity, but less evident than with FGF2 (Supplemental Figure S3).

To investigate downstream signaling, we performed western blot analysis on cells treated with erlotinib alone or in combination with FGF2 (Figure 3). Erlotinib treatment abolished phosphorylation of EGFR, Akt, and ERK in all cell lines. Phosphorylation of ERK was, however, partially restored in $PC9^{gFGFR1}$ and $HCC827^{gFGFR1}$ upon simultaneous erlotinib treatment and stimulation with FGF2 (Figure 3). Hence, FGF2 induced FGFR1 signaling seems to lead to decreased erlotinib-sensitivity coinciding with sustained ERK signaling.

### *FGFR1 Up-Regulation and AZD4547 Sensitivity*

FGFR1 overexpressing cells were previously shown to be sensitive to FGFR inhibitors *e.g.* AZD4547 [18,19]. Therefore, we hypothesized that $PC9^{gFGFR1}$ and $HCC827^{gFGFR1}$ cells may also be more sensitive to AZD4547 than $PC9^{gCTR}$ and $HCC827^{gCTR}$. Nevertheless, no difference in AZD4547 sensitivity was observed in $PC9^{gFGFR1}$ and $HCC827^{gFGFR1}$ compared to $PC9^{gCTR}$ and $HCC827^{gCTR}$ with or without addition of FGF2 (Figure 4, *A* and *B*). Hence, genetic up-regulation of FGFR1 does not lead to FGFR1-dependent growth in $PC9^{gFGFR1}$ and $HCC827^{gFGFR1}$ cells.

### *FGF2 Levels in EGFR Mutated Patients*

FGF2-presence was necessary to induce FGFR1-dependent erlotinib resistance in our *in vitro* experiments (Figure 2). We therefore hypothesized that FGF2 serum-levels could influence the TKI-response in EGFR-mutated patients. Based on the median

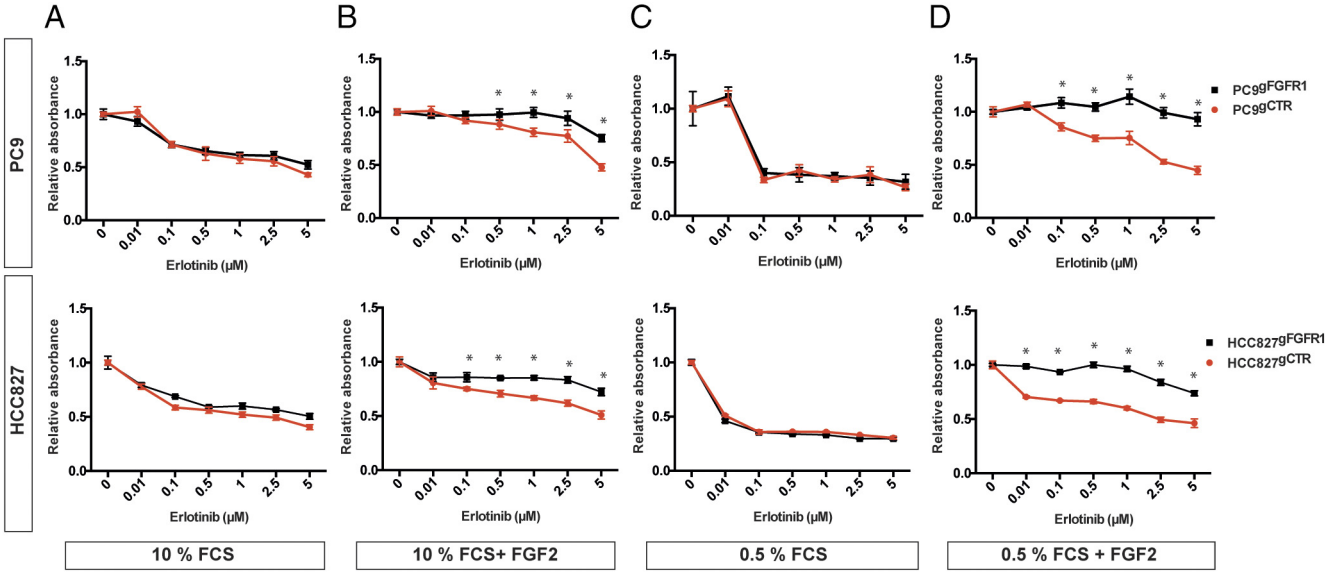


**Figure 2.** MTS analysis of erlotinib-sensitivity. A. Standard growth conditions. B. Standard growth conditions +20 ng/mL FGF2. C. Serum-starved conditions. D. Serum-starved conditions +20 ng/mL FGF2. Values were normalized to untreated control cells. * = $P < .005$ (N = 3).

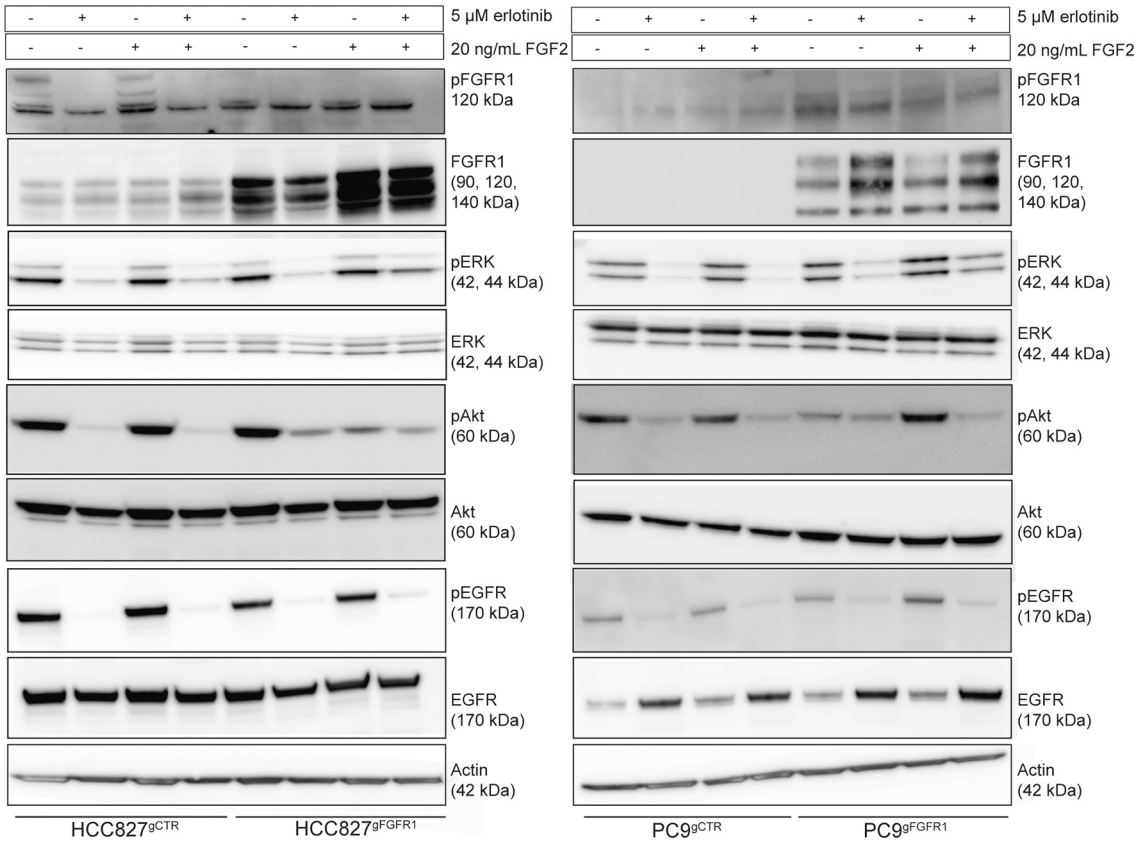


**Figure 3.** FGFR1 pathway analysis. Western blot analysis of cells grown in 0.5% FCS media with DMSO, 5 $\mu$M erlotinib, 20 ng/mL FGF2, or 5 $\mu$M erlotinib and 20 ng/mL FGF2 for 72 h (N = 2).

FGF2 level from FGF2 ELISA on 36 EGFR-mutated patients, we divided the patients into two groups and compared progression free survival (PFS) and overall survival (OS). There was no significant difference between the lower and higher FGF2 groups in accordance to PFS or OS (Figure 5, *A* and *B*).

### *EGFR TKI-Sensitivity in a Xenograft Mouse Model for NSCLC FGFR1 Up-Regulation*

PC9$^{gFGFR1}$ and PC9$^{gCTR}$ cells were inoculated into BALBc nu/nu mice for *in vivo* analysis to substantiate the differences in TKI-sensitivity seen *in vitro*. The two cell lines depicted even growth rates and there was a 100% successful inoculation rate. When tumors reached 100–200 mm$^3$, the mice were ranked after tumor size and randomized to erlotinib or vehicle treatment. During the 3 weeks of treatment there was significant differences between vehicle- and erlotinib-treated tumor sizes based on caliper measurements for PC9$^{gFGFR1}$ and PC9$^{gCTR}$ (Figure 6, *A* and *B*). At the end of the experiment, the tumors were resected, measured, and weighed. For the final tumor volume and weight, there was a significant difference between PC9$^{gCTR}$ tumors treated with vehicle and erlotinib (Figure 6, *C* and *E*). There was, however, not a significant difference between PC9$^{gFGFR1}$ vehicle- and erlotinib-treated tumors (Figure 6, *D* and *E*), which supports that PC9$^{gFGFR1}$ tumors were less sensitive to erlotinib.

### *Tumor Analyses*

To evaluate *FGFR1* mRNA expression and FGF2 levels during *in vivo* xenograft tumor growth, we performed qPCR and ELISA analyses on the resected tumors. *FGFR1* mRNA expression analysis confirmed a persistent *FGFR1* up-regulation in PC9$^{gFGFR1}$ xenografts (Figure 7*A*). No significant difference in *FGFR1* gene expression was observed between erlotinib- and vehicle-treated PC9$^{gFGFR1}$ xenografts (Figure 7*B*). Given that erlotinib specifically inhibits EGFR mutated cancer cells, we expected the relative contribution from PC9 cells to the tumor volume being decreased during erlotinib treatment. Therefore, we investigated the relative human cancer cell contribution to the tumor volume by calculating a human/mouse RNA ratio using species-specific *beta-actin* (*ACTB*) primers. This revealed a decreased human/mouse ratio in erlotinib-treated PC9$^{gCTR}$ tumors compared to vehicle-treated PC9$^{gCTR}$ tumors (Figure 7*C*). Hence, erlotinib treatment resulted in a decreased number of human cancer cells in accordance with an efficient erlotinib response in PC9$^{gCTR}$ cells. No significant difference in human/mouse ratio was observed between erlotinib- and vehicle-treated PC9$^{gFGFR1}$ tumors (Figure 7*C*). This finding supports inferior erlotinib response in PC9$^{gFGFR1}$ tumors.

All tumor samples had measurable levels of FGF2 (20–80 pg/μg protein) (Figure 7*D*). FGF2 levels in erlotinib-treated PC9$^{gFGFR1}$ tumors were lower than in vehicle-treated PC9$^{gFGFR1}$ tumors (Figure 7*D*). Such difference was not observed in erlotinib- and vehicle-treated PC9$^{gCTR}$ tumors (Figure 7*D*). For PC9$^{gFGFR1}$ tumors there were significant correlation between FGF2 level and final tumor size (Figure 7*E*). There was no such correlation in PC9$^{gCTR}$ tumors (Figure 7*F*).

## Discussion

FGFR1 is a tyrosine kinase receptor described as both a primary target in NSCLC and a mediator of TKI resistance [14,17,19,27,28]. The

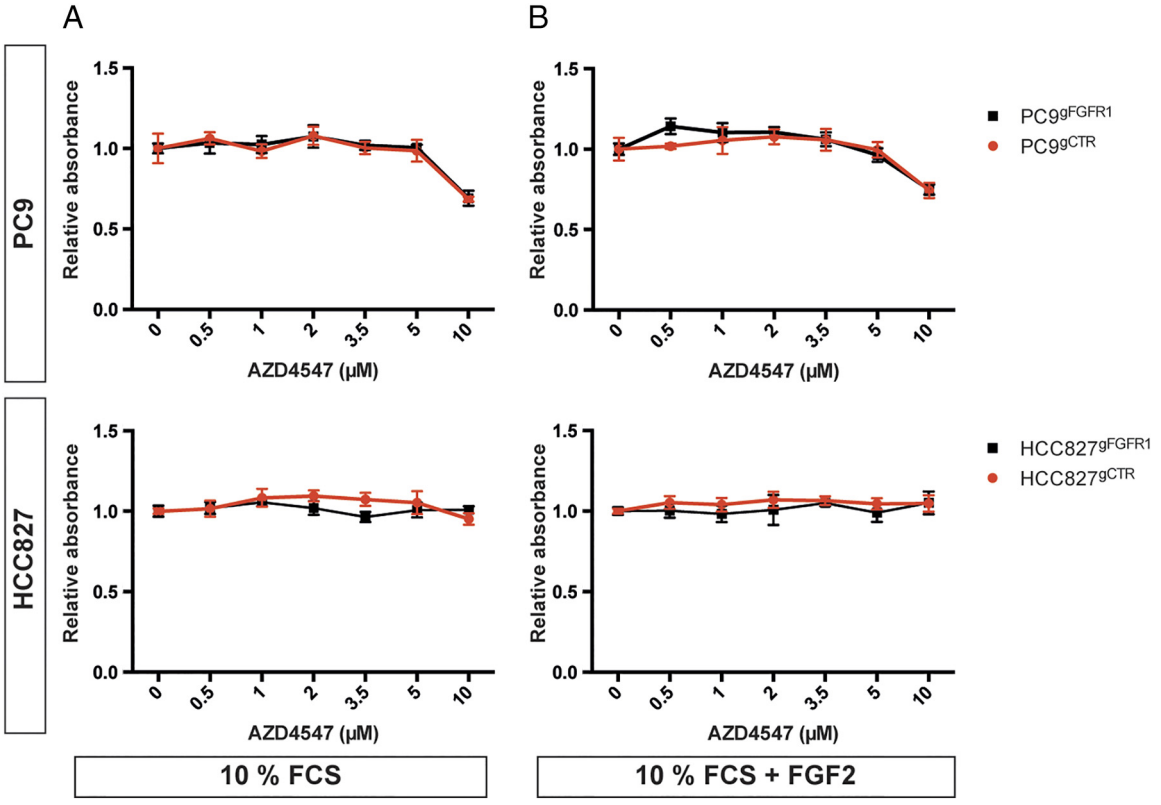


**Figure 4.** MTS analysis of AZD4547-sensitivity. A. Standard growth conditions. B. Standard growth conditions +20 ng/mL FGF2. Values were normalized to untreated control cells (N = 3).

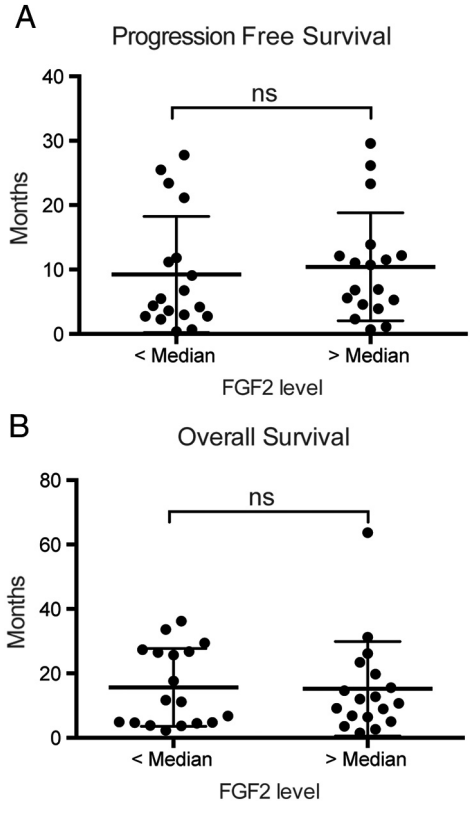


**Figure 5.** FGF2-levels analyzed with ELISA in EGFR-mutated patients. A. Progression free survival stratified by median FGF2-level. B. Overall survival stratified by median FGF2-level (n = 37).

importance of FGFR1-FGF2-dynamics has been highlighted for FGFR1 as a primary driver in NSCLC and as a mediator of acquired resistance to TKIs [16–18,29], but not in the setting of intrinsic TKI resistance. Here we investigated the FGFR1-FGF2 dynamics in relation to intrinsic TKI resistance in EGFR mutated NSCLC cell lines without or with CRISPR-dCas9-mediated up-regulation of FGFR1 expression. The CRISPR-dCas9 approach has several advantages compared to ectopic over-expression using cDNA-based plasmid or viral vectors. With the used CRISPR-dCas9 methodology, activating the genuine *FGFR1* promoter at physiological relevant transcriptional levels is obtainable. In addition, co- and post-transcriptional processing, as well as translation, of the up-regulated *FGFR1* RNA will follow the same routes as RNA for *FGFR1* normally does. Thereby, the induced up-regulation mimics FGFR1 up-regulation in NSCLC cells and at the same time allows experimental comparisons based on similar genetic backgrounds. The latter not achievable in comparisons of NSCLC cell lines with different basic FGFR1 expression levels.

In HCC827 and PC9 NSCLC cells, we found that FGFR1 up-regulation alone did not alter erlotinib-sensitivity. The presence of FGF2, however, decreased erlotinib-sensitivity in FGFR1-up-regulated cells *in vitro* and *in vivo*. Although this is the first report describing FGF2-FGFR1-mediated intrinsic EGFR TKI resistance, it is in accordance with studies of FGFR1 in other NSCLC settings. Malchers et al. showed that FGFR1-driven lung cancer cell lines depend on ligands, primarily FGF2, *in vitro* and *in vivo* [29]. In relation to FGFR1 as a mediator of acquired erlotinib-resistance, a FGF2-FGFR1 autocrine loop has been reported as well [16–18]. In the acquired resistance studies, FGF2 and FGFR1 were both up-

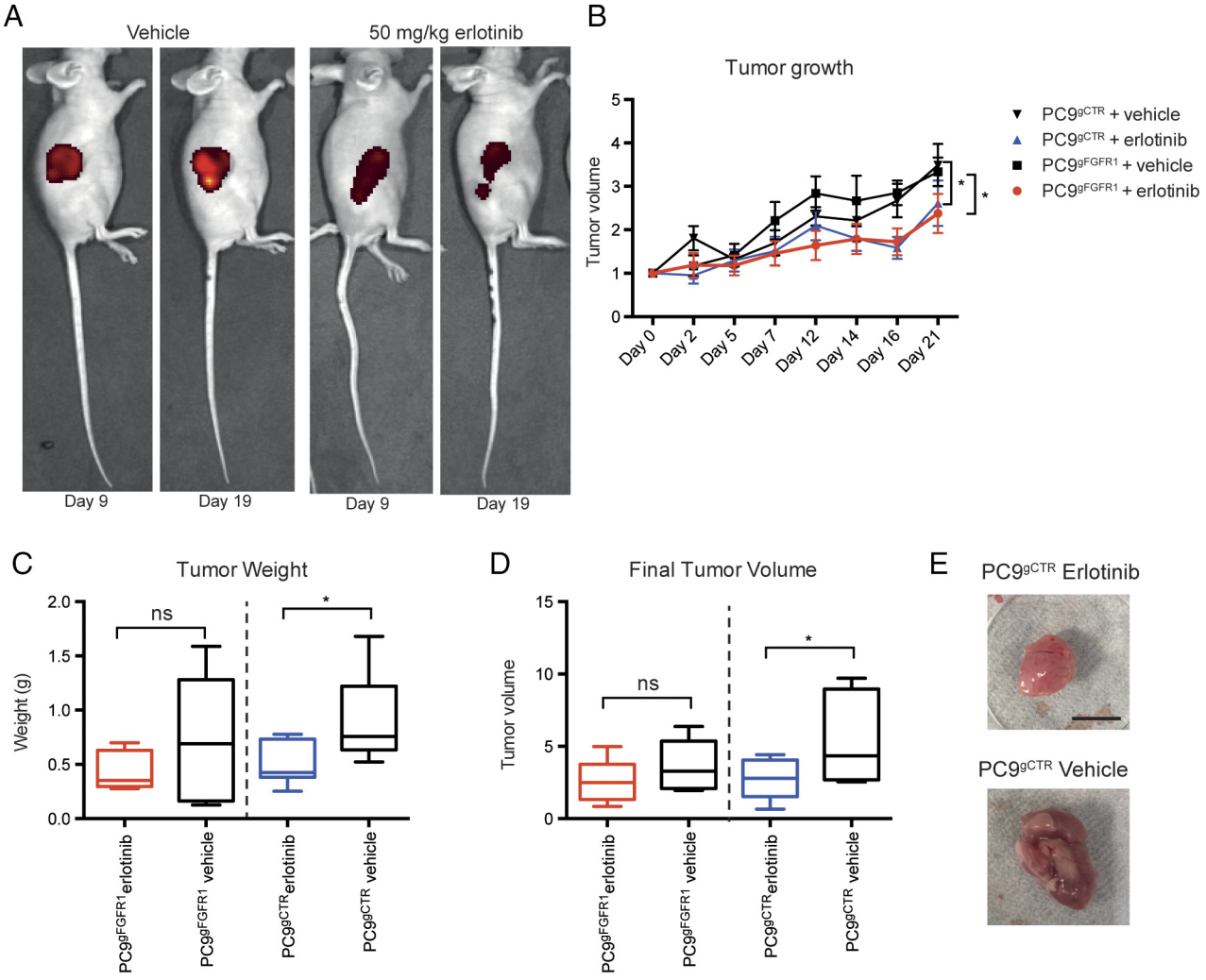


**Figure 6.** *In vivo* study of erlotinib-sensitivity. A. Representative PC9$^{gFGFR1}$ xenografted mice treated with vehicle or erlotinib. B. Tumor growth measured by caliper in PC9$^{gFGFR1}$ and PC9$^{gCTR}$ treated with vehicle or erlotinib (n (erlotinib) = 8, n (vehicle) = 7). Tumor volumes are normalized to the volume measured on day 0 (treatment start). * = $P < .05$. C. Final tumor weight after resection, ns = nonsignificant, * $P = .03$. D. Final tumor volume of resected tumors normalized to measured volume on day 0, ns = nonsignificant, * $P = .0235$. E. Representative tumors from PC9$^{gCTR}$ treated with vehicle or erlotinib. Inserted black bar represents 10 mm.

regulated during resistance development [16–18]. Here, we observed that exogenous FGF2 addition was needed to alter the erlotinib sensitivity of NSCLC cells with genetic FGFR1 up-regulation.

*In vivo* we observed a significant difference in size between erlotinib- and vehicle-treated PC9$^{gCTR}$ xenografted tumors, a difference not present in PC9$^{gFGFR1}$ tumors. Gene expression analysis revealed a persistent *FGFR1* gene up-regulation in PC9-$^{gFGFR1}$ at the end of the *in vivo* experiment in both vehicle- and erlotinib-treated mice. Analyses of human/mouse RNA-ratios in the tumors revealed decreased contribution from human cancer cells in erlotinib-treated PC9$^{gCTR}$ xenografts compared to vehicle treated, supporting a pronounced erlotinib-induced PC9$^{gCTR}$ cell death. In addition, the increased mouse cell contribution may have led to an overestimated tumor size in erlotinib-treated PC9$^{gCTR}$ xenografts during the experiment. We measured the FGF2 levels in the tumor tissue and observed FGF2 levels in the order of 20–80 pg/μg protein for all tumor samples. The FGF2 levels correlated with tumor size in PC9$^{gFGFR1}$ xenografts, but not in PC9$^{gCTR}$ xenografts suggesting a role for the FGF2-FGFR1 pathway in tumor growth. For PC9$^{gCTR}$ tumors FGF2 levels in the erlotinib treated tumor group was higher than expected. This could be a consequence of a higher degree of mouse cell infiltration. We also observed presence of significantly lower FGF2 levels in erlotinib-treated PC9$^{gFGFR1}$ xenografts compared to vehicle-treated PC9$^{gFGFR1}$ xenografts. This difference in FGF2-levels could indicate a greater turnover of FGF2 in the tumors caused by FGF2-internalization upon receptor-binding or may partly be due to a tendency towards larger sizes of vehicle tumors (Figure 5*D*) [30].

Due to the critical role of FGF2 in *in vitro* and *in vivo* FGFR1-mediated erlotinib resistance, we evaluated if FGF2 expression measurements could have a prognostic and predictive value in a cohort of 36 EGFR-mutated NSCLC patients treated with erlotinib. FGF2 has previously been investigated as a biomarker in advanced NSCLC, but not in a cohort containing only EGFR-mutated patients [31]. There was no difference in OS or PFS, when the patients were stratified by median FGF2 expression level. Hence, FGF2 alone was not a predictor of OS or PFS. However, to clearly elucidate the potential role of FGF2 as a marker of intrinsic EGFR-TKI resistance

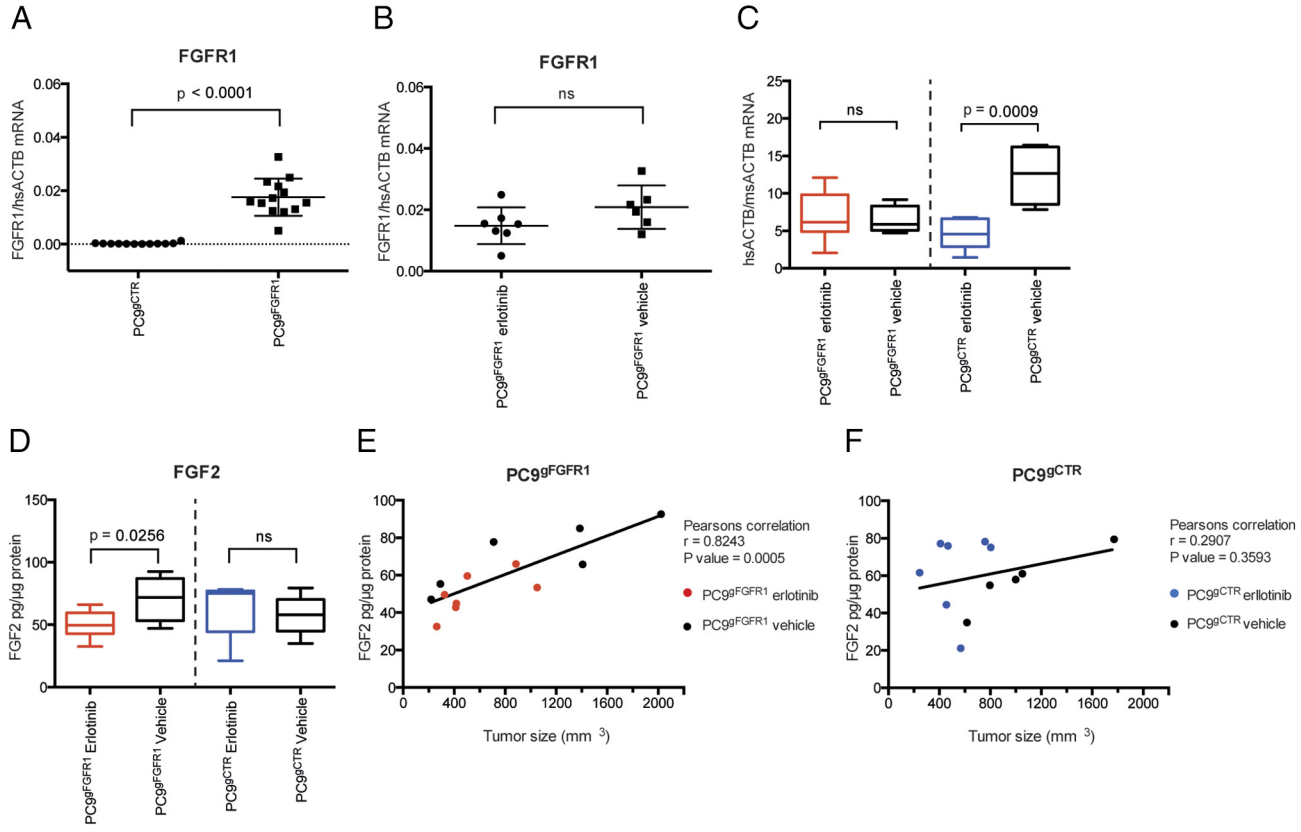


**Figure 7.** Xenografted tumor analyses. A. *FGFR1* gene expression analysis of all samples (n (erlotinib) = 8, n (vehicle) = 7). B. *FGFR1* gene expression analysis of PC9$^{gFGFR1}$ tumors. C. Human beta-actin (hsACTB) expression divided into treatment groups. D. FGF2-levels analyzed with ELISA divided by treatment group (n (PC9$^{gFGFR1}$erlotinib) = 7, n (PC9$^{gFGFR1}$ vehicle) = 5, n (PC9$^{gCTR}$ erlotinib) = 8, n (PC9$^{gCTR}$ vehicle) = 7). Correlation of FGF2 levels and final tumor volume in E. PC9$^{gFGFR1}$ tumors and F. PC9$^{gCTR}$ (n (PC9$^{gFGFR1}$erlotinib) = 7, n (PC9$^{gFGFR1}$ vehicle) = 5, n (PC9$^{gCTR}$ erlotinib) = 8, n (PC9$^{gCTR}$ vehicle) = 7).

in EGFR-mutated NSCLC, FGF2 levels must be accessed in a larger cohort of EGFR-mutated patients treated with EGFR-TKI and preferentially matched with FGFR1 expression data. Overall, our study suggests that FGFR1 expression in EGFR-mutated NSCLC enables intrinsic resistance to erlotinib, and points to the necessity of investigating the combinatorial value of FGF2 and FGFR1 as biomarkers for intrinsic EGFR TKI resistance in EGFR-mutated NSCLC.

Supplementary data to this article can be found online at https://doi.org/10.1016/j.tranon.2018.11.017.

## Competing Interests

The authors have no conflicting interests.

## Acknowledgements

We thank the Animal Facility, Department of Biomedicine, at Aarhus University for assisting with animal handling. This project was supported by Dagmar Marshalls Mindelegat, Fabrikant Einar Willumsens Mindelegat, Marie og Børge Kroghs Fond, P. A. Messerschmidt og Hustrus Fond, Thora og Viggo Grove's Mindelegat, and Familien Erichsens Familiefond.

## References

[1] IARC (2014). I.A. for R. on Cancer, World Cancer Report 2014; 2014 .

[2] Goldstraw P, Chansky K, Crowley J, Rami-Porta R, Asamura H, Eberhardt WEE, Nicholson AG, Groome P, Mitchell A, and Bolejack V (2016). International Association for the Study of Lung Cancer Staging and Prognostic Factors Committee, Advisory Boards, and Participating Institutions; International Association for the Study of Lung Cancer Staging and Prognostic Factors Committee Advisory Boards and Participating Institutions. *J Thorac Oncol* **11**, 39–51. http://dx.doi.org/10.1016/j.jtho.2015.09.009.

[3] Bos M, Gardizi M, Schildhaus H-U, Buettner R, and Wolf J (2013). Activated RET and ROS: two new driver mutations in lung adenocarcinoma. *Transl Lung Cancer Res* **2**, 112–121. http://dx.doi.org/10.3978/j.issn.2218-6751.2013.03.08.

[4] Sullivan I and Planchard D (2016). ALK inhibitors in non-small cell lung cancer: the latest evidence and developments. *Ther Adv Med Oncol* **8**, 32–47. http://dx.doi.org/10.1177/1758834015617355.

[5] Kazandjian D, Blumenthal GM, Yuan W, He K, Keegan P, and Pazdur R (2016). FDA approval of gefitinib for the treatment of patients with metastatic EGFR mutation-positive non-small cell lung cancer. *Clin Cancer Res* **22**. http://dx.doi.org/10.1158/1078-0432.CCR-15-2266.

[6] Sequist LV, Joshi VA, Jänne PA, Muzikansky A, Fidias P, Meyerson M, Haber DA, Kucherlapati R, Johnson BE, and Lynch TJ (2007). Response to treatment and survival of patients with non-small cell lung cancer undergoing somatic EGFR mutation testing. *Oncologist* **12**, 90–98.

[7] Weber B, Hager H, Sorensen BS, McCulloch T, Mellemgaard A, Khalil AA, Nexo E, and Meldgaard P (2014). EGFR mutation frequency and effectiveness of erlotinib: a prospective observational study in Danish patients with non-small cell lung cancer. *Lung Cancer* **83**, 224–230. http://dx.doi.org/10.1016/j.lungcan.2013.11.023.

[8] Lynch TJ, Bell DW, Sordella R, Gurubhagavatula S, Okimoto RA, Brannigan BW, Harris PL, Haserlat SM, Supko JG, and Haluska FG, et al (2004). Activating mutations in the epidermal growth factor receptor underlying responsiveness of non-small-cell lung cancer to gefitinib. *N Engl J Med* **350**, 2129–2139. http://dx.doi.org/10.1056/NEJMoa040938.

[9] Felip E, Gridelli C, Baas P, Rosell R, Stahel R, and Members P (2011). Metastatic non-small-cell lung cancer: consensus on pathology and molecular

tests, first-line, second-line, and third-line therapy 1st ESMO Consensus Conference in Lung Cancer; Lugano 2010. *Ann Oncol* **22**, 1507–1519. http://dx.doi.org/10.1093/annonc/mdr150.

[10] Cortot AB and Janne PA (2014). Molecular mechanisms of resistance in epidermal growth factor receptor-mutant lung adenocarcinomas. *Eur Respir Rev* **23**, 356–366. http://dx.doi.org/10.1183/09059180.00004614.

[11] Jackman D, Pao W, Riely GJ, Engelman J a, Kris MG, Jänne P a, Lynch T, Johnson BE, and Miller V a (2010). Clinical definition of acquired resistance to epidermal growth factor receptor tyrosine kinase inhibitors in non-small-cell lung cancer. *J Clin Oncol* **28**, 357–360. http://dx.doi.org/10.1200/JCO.2009.24.7049.

[12] Winther Larsen A, Nissen PH, Meldgaard P, Weber B, and Sorensen BS (2014). EGFR CA repeat polymorphism predict clinical outcome in EGFR mutation positive NSCLC patients treated with erlotinib. *Lung Cancer* **85**, 435–441. http://dx.doi.org/10.1016/j.lungcan.2014.06.016.

[13] Costa C, Molina MA, Drozdowskyj A, Giménez-Capitán A, Bertran-Alamillo J, Karachaliou N, Gervais R, Massuti B, Wei J, and Moran T, et al (2014). The impact of EGFR T790M mutations and BIM mRNA expression on outcome in patients with EGFR-mutant NSCLC treated with erlotinib or chemotherapy in the randomized phase III EURTAC trial. *Clin Cancer Res* **20**, 2001–2010. http://dx.doi.org/10.1158/1078-0432.CCR-13-2233.

[14] Zhang X, Zhang J, Li M, Huang X, Yang X, Zhong W, Xie L, Zhang L, Zhou M, and Gavine P, et al (2013). Establishment of patient-derived non-small cell lung cancer xenograft models with genetic aberrations within EGFR, KRAS and FGFR1: useful tools for preclinical studies of targeted therapies. *J Transl Med* **11**, 168. http://dx.doi.org/10.1186/1479-5876-11-168.

[15] Sharifnia T, Rusu V, Piccioni F, Bagul M, Imielinski M, Cherniack AD, Pedamallu CS, Wong B, Wilson FH, and Garraway LA, et al (2014). Genetic modifiers of EGFR dependence in non-small cell lung cancer. *Proc Natl Acad Sci* **111**, 18661–18666. http://dx.doi.org/10.1073/pnas.1412228112.

[16] Terai H, Soejima K, Yasuda H, Nakayama S, Hamamoto J, Arai D, Ishioka K, Ohgino K, Ikemura S, and Sato T, et al (2013). Activation of the FGF2-FGFR1 autocrine pathway: A novel mechanism of acquired resistance to gefitinib in NSCLC. *Mol Cancer Res* **11**, 759–767. http://dx.doi.org/10.1158/1541-7786.MCR-12-0652.

[17] Azuma K, Kawahara A, Sonoda K, Nakashima K, Tashiro K, Watari K, Izumi H, Kage M, Kuwano M, and Ono M, et al (2014). FGFR1 activation is an escape mechanism in human lung cancer cells resistant to afatinib, a pan-EGFR family kinase inhibitor. *Oncotarget* **5**, 5908–5919. http://dx.doi.org/10.18632/oncotarget.1866.

[18] Ware KE, Hinz TK, Kleczko E, Singleton KR, Marek L a, Helfrich B a, Cummings CT, Graham DK, Astling D, and Tan a-C, et al (2013). A mechanism of resistance to gefitinib mediated by cellular reprogramming and the acquisition of an FGF2-FGFR1 autocrine growth loop. *Oncogenesis* **2**, e39. http://dx.doi.org/10.1038/oncsis.2013.4.

[19] Jakobsen KR, Demuth C, Madsen AT, Hussmann D, Vad-Nielsen J, Nielsen AL, and Sorensen BS (2017). MET-Amplification and epithelial-to-mesenchymal transition exist as parallel resistance mechanisms in erlotinib-resistant HCC827 non small-cell lung cancer cells. *Oncogenesis* **6**(4), e307. http://dx.doi.org/10.1038/oncsis.2017.17.

[20] Ornitz DM and Itoh N (2015). The fibroblast growth factor signaling pathway. *Wiley Interdiscip Rev Dev Biol* **4**, 215–266. http://dx.doi.org/10.1002/wdev.176.

[21] Beenken A and Mohammadi M (2009). The FGF family: biology, pathophysiology and therapy. *Nat Rev Drug Discov* **8**, 235–253. http://dx.doi.org/10.1038/nrd2792.

[22] Wang K, Ji W, Yu Y, Li Z, Niu X, Xia W, and Lu S (2018). FGFR1-ERK1/2-SOX2 axis promotes cell proliferation, epithelial-mesenchymal transition, and metastasis in FGFR1-amplified lung cancer. *Oncogene* **37**(39), 5340–5354. http://dx.doi.org/10.1038/s41388-018-0311-3.

[23] Konermann S, Brigham MD, Trevino AE, Joung J, Abudayyeh OO, Barcena C, Hsu PD, Habib N, Gootenberg JS, and Nishimasu H, et al (2014). Genome-scale transcriptional activation by an engineered CRISPR-Cas9 complex. *Nature* **517**, 583–588. http://dx.doi.org/10.1038/nature14136.

[24] Vad-Nielsen J, Lin L, Bolund L, Nielsen AL, and Luo Y (2016). Golden Gate Assembly of CRISPR gRNA expression array for simultaneously targeting multiple genes. *Cell Mol Life Sci* **73**, 4315–4325. http://dx.doi.org/10.1007/s00018-016-2271-5.

[25] Vad-Nielsen J, Nielsen AL, and Luo Y (2018). Simple method for assembly of CRISPR synergistic activation mediator gRNA expression array. *J Biotechnol* **274**, 54–57. http://dx.doi.org/10.1016/j.jbiotec.2018.03.018.

[26] Thomsen R, Sølvsten CAE, Linnet TE, Blechingberg J, and Nielsen AL (2010). Analysis of qPCR data by converting exponentially related Ct values into linearly related X0 values. *J Bioinform Comput Biol* **8**, 885–900. http://dx.doi.org/10.1142/S0219720010004963.

[27] Paik PK, Shen R, Berger MF, Ferry D, Soria JC, Mathewson A, Rooney C, Smith NR, Cullberg M, and Kilgour E, et al (2017). A phase Ib open-label multicenter study of AZD4547 in patients with advanced squamous cell lung cancers. *Clin Cancer Res* **23**, 5366–5373. http://dx.doi.org/10.1158/1078-0432.CCR-17-0645.

[28] Weiss J, Sos ML, Seidel D, Peifer M, Zander T, Heuckmann JM, Ullrich RT, Menon R, Maier S, and Soltermann A, et al (2010). Frequent and focal FGFR1 amplification associates with therapeutically tractable FGFR1 dependency in squamous cell lung cancer. *Sci Transl Med* **2**. http://dx.doi.org/10.1126/scitranslmed.3001451.

[29] Malchers F, Dietlein F, Schöttle J, Lu X, Nogova L, Albus K, Fernandez-Cuesta L, Heuckmann JM, Gautschi O, and Diebold J, et al (2014). Cell-autonomous and non-cell-autonomous mechanisms of transformation by amplified FGFR1 in lung cancer. *Cancer Discov* **4**, 246–257. http://dx.doi.org/10.1158/2159-8290.CD-13-0323.

[30] Facchiano A, Russo K, Facchiano AM, De Marchis F, Facchiano F, Ribatti D, Aguzzi MS, and Capogrossi MC (2003). Identification of a novel domain of fibroblast growth factor 2 controlling its angiogenic properties. *J Biol Chem* **278**, 8751–8760. http://dx.doi.org/10.1074/jbc.M209936200.

[31] Hu M, Hu Y, He J, and Li B (2016). Prognostic value of basic fibroblast growth factor (bFGF) in lung cancer: A systematic review with meta-analysis. *PLoS One* **11**, 1–14. http://dx.doi.org/10.1371/journal.pone.0147374.